

Green Chemistry

Cutting-edge research for a greener sustainable future

Accepted Manuscript

View Article Online
View Journal

This article can be cited before page numbers have been issued, to do this please use: K. Hiroishi, H. Matsumoto, H. Kasai, M. Nagao, E. Nishibori and Y. Miura, *Green Chem.*, 2026, DOI: 10.1039/D5GC05291B.



This is an Accepted Manuscript, which has been through the Royal Society of Chemistry peer review process and has been accepted for publication.

Accepted Manuscripts are published online shortly after acceptance, before technical editing, formatting and proof reading. Using this free service, authors can make their results available to the community, in citable form, before we publish the edited article. We will replace this Accepted Manuscript with the edited and formatted Advance Article as soon as it is available.

You can find more information about Accepted Manuscripts in the [Information for Authors](#).

Please note that technical editing may introduce minor changes to the text and/or graphics, which may alter content. The journal's standard [Terms & Conditions](#) and the [Ethical guidelines](#) still apply. In no event shall the Royal Society of Chemistry be held responsible for any errors or omissions in this Accepted Manuscript or any consequences arising from the use of any information it contains.

Green foundation box

1. This work introduces a mechanochemistry-directed design of polymer-supported organocatalyst for solvent-less organic synthesis, which demonstrates a green and sustainable practice for chiral compounds via solvent reduction and improvement of catalytic performance.
2. The methodology can avoid bulk solvents, shorten reaction time, and prolong catalytic durability for mechanochemical organic synthesis of fine chemicals with a ball mill. Compared with small-molecular catalyst, our polymer-supported catalyst can dramatically accelerate catalytic reaction with durable catalytic lifetime. Furthermore, the E-factor of the polymer catalyst system was much lower (0.1) than that of solution-based system (57), aligning with green chemistry principles by solvent usage reduction and catalyst lifetime improvement.
3. Further greening can include development of fully solvent-free asymmetric reaction and extending the strategy to continuous-flow mechanochemistry with twin-screw extrusion, enhancing scalability and sustainability.



ARTICLE

Solvent-less mechanochemical asymmetric reactions in a ball mill utilizing polymer-supported Hayashi-Jørgensen catalyst: effect of polymer backbone and flexibility on its catalytic performanceKento Hiroishi,^a Hikaru Matsumoto,^{*a} Hidetaka Kasai,^b Masanori Nagao,^a Eiji Nishibori,^c and Yoshiko Miura^{**a}

Fine chemical synthesis under solvent-free or solvent-less mechanochemical conditions are highly desirable from a green chemistry perspective. However, the inherent low contact efficiency between the catalyst and solid substrates often results in low reaction efficiency. Polymer-assisted grinding (POLAG) in a ball mill has been developed for the solvent-less organic synthesis, where polymers are used as additives to effectively disperse solid reactants. Specifically, polymer-supported catalysts have been shown to function as the POLAG additives to enhance catalytic performance. However, effects of the structures of the polymer-supported catalysts on their catalytic performance has not been fully investigated. Here, we prepared polymer-supported catalysts bearing Hayashi-Jørgensen catalyst with different polymer backbones and chemical structures of spacer monomers. In asymmetric Michael addition reaction in the presence of solid reactants with a ball mill, the polymer-supported catalyst exhibited a significantly higher turnover number compared to its small molecule counterpart. Additionally, a correlation between glass transition temperature of the polymer-supported catalyst and turnover frequency was confirmed, which suggested that the flexible polymer support facilitated the solid dispersion and boosted subsequent catalytic cycles.

Received 00th January 20xx,
Accepted 00th January 20xx

DOI: 10.1039/x0xx00000x

Introduction

Recently, sustainable development goals (SDGs) have attracted global attention. This focus has been extended to chemical production, where green chemistry is strongly related to the SDGs for environmentally benign synthetic processes.¹ Among the 12 principles of green chemistry, waste prevention is paramount. On the other hand, the present fine chemical synthesis generates a large amount of waste such as byproducts and solvents due to its complicated synthetic routes, low productivity and selectivity. In particular, the solvent wastes account for approximately 90% of reagents used through the fine chemical productions.^{2,3} As a key metric for the green chemistry, E-factor can reach up to 10² kg-waste kg-product⁻¹ in the fine chemical synthesis, which is rather higher than that in bulk chemical synthesis (1–5 kg-waste kg-product⁻¹).⁴ Thus, reduction of solvent usage in the fine chemical productions is crucial to achieve SDGs by suppression of environmental footprints through green synthetic processes.

Mechanochemistry is a discipline that deals with physical and chemical changes induced by mechanical forces such as compression, shear, and friction in small molecules,^{5–8} crystals,^{9,10} and polymers.^{11–13} Recent progress in the mechanochemical protocol has witnessed the utilization of mechanochemistry in the organic synthesis, which is termed as “mechanochemical organic synthesis.”^{5,14} The mechanochemical organic synthesis are driven by mechanical energy input by sonication¹³ and physical grinding.^{16,17} Unlike traditional solution processes, ball milling processes have attracted considerable attention owing to its solvent-less conditions, shorter reaction time, and unique reactivity and selectivity.^{16,17} In the ball mill, mechanical energy is transferred to substrates and catalysts by collision and friction at surface of balls and inner wall of jar during shaking or revolution (Fig 1a). To date, numerous reports have demonstrated the advantages of solvent-less mechanochemical organic synthesis such as reduced solvents usage, accelerated reaction rates, and efficient conversion of hardly soluble reactants.^{7,8}

One unique advantage of the mechanochemical organic synthesis is that the solid-state organic reactions can be promoted under solvent-less conditions. In this system, mixing efficiency is strongly correlated with the resultant reaction performance. This is primarily due to limited contact efficiency at substrate-substrate and substrate-catalyst interfaces in the solid-state systems compared to the conventional solution systems (Fig. 1a).¹⁶ In this sense, previous studies have shown that additives could improve the mixing efficiency and the reaction yields. Liquid-assisted grinding (LAG) is one of the

^a Department of Chemical Engineering, Faculty of Engineering, Kyushu University, 744 Motooka, Nishi-ku, Fukuoka 819-0395, Japan Address here.

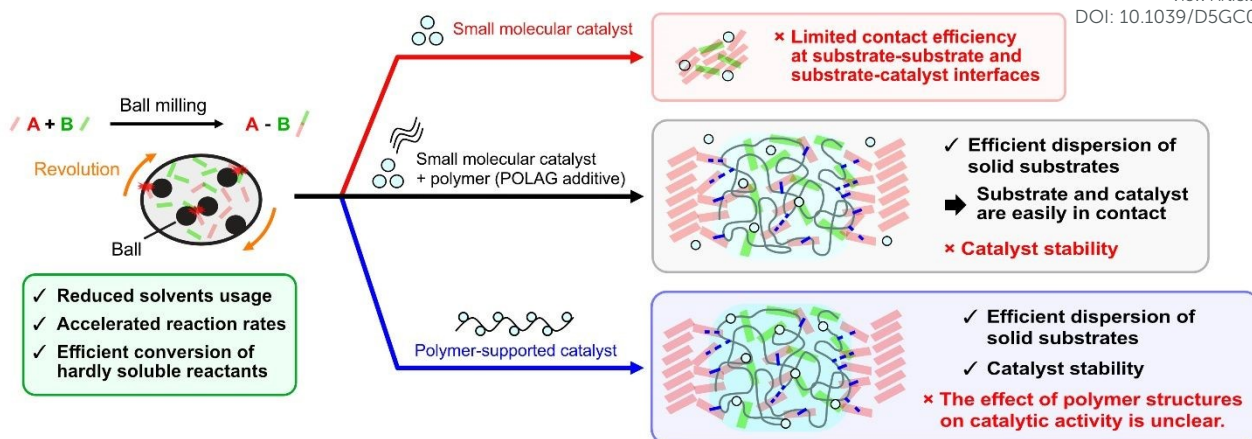
^b Department of Materials Science, Osaka Metropolitan University, 1-1 Gakuen-cho, Naka-ku, Sakai, Osaka 599-8531, Japan

^c Department of Physics, Institute of Pure and Applied Sciences and Tsukuba Research Center for Energy Materials Science, University of Tsukuba, Tsukuba 305-8571, Japan

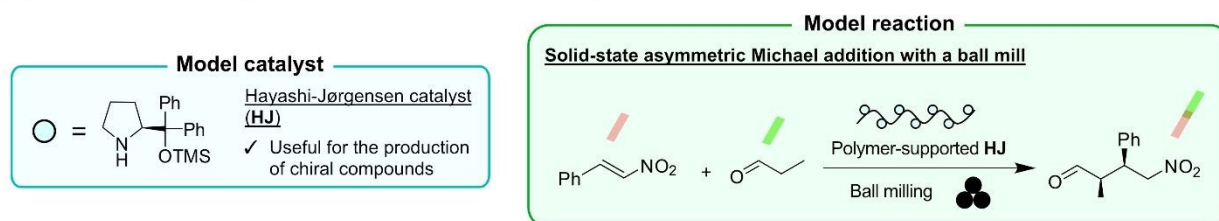
† Electronic supplementary information (ESI) available: Materials and methods, synthetic procedures, EDX and thermographic analyses, and NMR spectra. See DOI: 10.1039/x0xx00000x



(a) Mechanochemical organic synthesis with a ball mill



(b) The model catalyst and reaction in this study



(c) Chemical structures of polymer-supported HJ

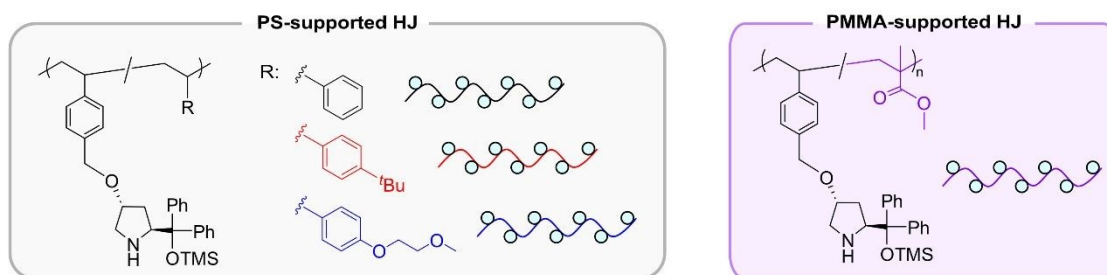


Fig. 1 (a) Mechanochemical organic synthesis with a ball mill. (b) The model catalyst (HJ) and reaction (solid-state asymmetric Michael addition with a ball mill) in this study. (c) Chemical structures of polymer-supported HJ.

strategies to alter the reactivity and selectivity by adding trace amount of liquid ($< 2 \mu\text{L}$ -liquid $\text{mg}\cdot\text{solid}^{-1}$).¹⁸⁻²⁰ It has been recognized that the LAG could promote partial dissolution of the solid substrate at the surfaces and increase its molecular mobility, resulting in dramatic improvement of the mixing and reaction efficiencies.²¹ Another method is known as polymer-assisted grinding (POLAG), in which polymers are used as additives. For instance, Lamaty and co-workers reported the synthesis of pharmaceutical ethotoin from solid substrates using poly(ethyleneglycol) (PEG).^{22,23} They also reported the application of the PEG additive to Pd-catalyzed Mizoroki-Heck reactions under solvent-free conditions.²⁴ Kubota and Ito reported Pd-catalyzed Suzuki-Miyaura cross-couplings in the presence of solid substrates by utilizing poly(tetrafluoroethylene) (PTFE) additive.²⁵ These pioneer researches on the use of POLAG to solid-state mechanochemical organic synthesis suggest that substrate-polymer interactions at their interfaces could efficiently

disperse the solid substrates and subsequently accelerate the reactions.

Merger of the POLAG strategy and excellent catalytic systems have seen its significant advancement in the solid-state mechanochemical organic synthesis. For example, Kubota and Ito developed phosphine-Pd catalyst covalently bound to PEG as efficient catalytic system in solid-state Suzuki-Miyaura cross-couplings. This phosphine-PEG hybrid material featured well dispersion of solid substrates and effective suppression of Pd aggregation in the flexible PEG chains.²⁶ Yu and co-workers reported regioselective Heck reactions using cyclodextrin (CD)-supported Pd catalysts by leveraging the substrate inclusion properties of the CD matrix.²⁷ The catalyst reactivity and selectivity was significantly altered by placing the catalyst and polymer in close proximity, thereby enabling cooperative effect for efficient solid substrate dispersion, metal catalyst stabilization, and selective molecular transformations (Fig. 1a). Thus, the mechanochemistry-directed catalyst design featuring



unique polymer properties provides green synthetic protocols with unprecedented reactivity and selectivity. To this end, it is important to understand the polymer-supported catalyst system in the solid-state mechanochemical organic synthesis. However, deep insights are still lacking. For example, effects of polymer structure on catalytic performance have not been systematically investigated yet, which lead to design guidelines for efficient solvent-less organic synthesis and thereby contribute to green chemistry.

Herein, we systematically elucidated the influence of polymer support structures on catalytic performance in solid-state mechanochemical synthesis. As a model catalyst, Hayashi-Jørgensen catalyst (**HJ**) was selected, as it is useful asymmetric organocatalyst for the synthesis of fine chemicals such as chiral γ -amino acid derivatives (Fig. 1b). The utility of the **HJ** has been demonstrated not only in solution process^{28,29} but also the mechanochemical process with ball mill.³⁰ In addition, the incorporation of the **HJ** moiety into synthetic polymers have been reported.^{31–33} In this study, the polymer-supported **HJ** was synthesized through a simple radical copolymerization of vinylated **HJ** with spacer monomer (Fig. 1b). To vary the structures of the polymer, different chemical structures of the spacer monomers were copolymerized. Using the polymer catalyst, asymmetric Michael addition of aldehyde to nitroalkene was performed under solvent-less conditions using a planetary ball mill (Fig. 1b). In situ powder X-ray diffraction (PXRD) analysis during the ball milling was performed to monitor the solid state of the reaction mixture. Comparative experiments with small molecule counterparts were performed to highlight the superior catalytic performance of the polymer-supported **HJ**. Through the systematic investigation of the series of polymer catalysts, we found the correlation between the chemical structure of the spacer monomer and catalytic performance, which was explained by flexibility of the polymer-supported catalyst. Furthermore, green chemistry metrics (e.g. E-factor, process mass intensity (PMI), and solvent intensity (SI)) were estimated in the present catalytic system for contribution of the polymer-supported **HJ** to the sustainable and green organic synthesis through waste prevention.

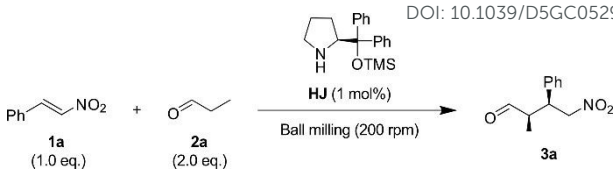
Result and discussion

Reaction condition screening for Michael addition with a ball mill

We first screened the mechanochemical conditions for the Michael addition reaction between (E)- β -nitrostyrene (**1a**) and propionaldehyde (**2a**). The reactants were placed in a ZrO₂ milling jar with ZrO₂ balls and milled in a planetary ball mill. After 4 h, the milling was stopped followed by opening the jar to analyze the reaction mixture. In the absence of **HJ**, no generation of product (**3a**) from the Michael addition was observed (Entry 1, Table 1). On the other hand, the addition of **HJ** achieved a significant conversion to the product (51% yield, Entry 2). At different revolution rates (200 and 400 rpm), no significant difference in the yields was observed (51 and 41%, respectively, Entries 2 and 3). Both conditions showed excellent

Table 1 Screening of reaction conditions for asymmetric Michael addition reactions^a

DOI: 10.1039/D5GC05291B



Entry	Revolution rate [rpm]	Reaction time [h]	Catalyst [mol%]	Yield [%] ^c	syn/anti ^c
1	200	4	–	Trace	n.d.
2	200	4	1	51	94:6
3	400	4	1	41	87:13
4	200	4	5	99	65:35
5	200	4	10	94	67:33
6 ^b	–	24	1	38	94:6

^a Reaction condition: **1a** (1.8 mmol, 1.0 eq.), **2a** (3.6 mmol, 2.0 eq.) and **HJ** were milled in 20 mL ZrO₂ jar with four ZrO₂ balls (Φ = 10 mm) under an ambient atmosphere. ^b Reaction condition: **1a** (1.8 mmol, 1.0 eq.), **2a** (3.6 mmol, 2.0 eq.), and **HJ** were stirred in toluene (9 mL) at 25°C with a magnetic stirring bar. ^c Determined by HPLC.

diastereoselectivity, indicating stereoselective reaction with ball mill (94:6 and 87:13 *syn/anti*, respectively, Entries 2 and 3). However, a black powder was observed in the reaction mixture processed at 400 rpm (Fig. S2a–c†). An energy dispersive X-ray spectroscopy (EDX) analysis revealed that this powder was mainly composed of Zr (Fig. S2d†). This suggested that ZrO₂ powder from the jar and balls contaminated the reaction mixture due to vigorous milling and abrasion. No abrasion of the jar or balls occurred at 200 rpm. Thermographic analysis showed that the temperature of the reaction mixture was approximately 30°C immediately after opening the milling jar (Fig. S3†). This confirmed that there was no excessive heat generation and reaction promotion under the ball milling condition.

By fixing the revolution rate at 200 rpm and increasing the catalyst loading to 5 and 10 mol%, the yields increased to 99 and 94%, respectively (Entries 4 and 5). On the other hand, a decrease in stereoselectivity was observed (65:35 and 67:33 *syn/anti*), suggesting that an increase in the contact frequency between **3a** and **HJ** induced epimerization.³² For comparison, the Michael addition reaction was performed in a solution process with toluene as a reaction solvent. Even after 24 h, the Michael addition in the toluene gave lower yield (38%, Entry 6). The optimization of the reaction conditions using a ball mill allowed for the rapid and stereoselective mechanochemical organic synthesis, which highlighted the usefulness of solvent-less molecular transformations.

In situ analysis of reaction mixture during ball milling

To clarify the state of the reaction mixture under ball milling, in situ PXRD was performed (Fig. S4, for details, see ESI†).^{34,35} A broad peak at 2θ = 5.5° was observed due to scattering from a polycarbonate (PC) milling jar used in all the in situ PXRD analyses (Fig. 2). A mixture of **1a** and **2a** (**1a** + **2a**) was processed with the ball mill. In the in situ PXRD pattern of **1a** + **2a**,



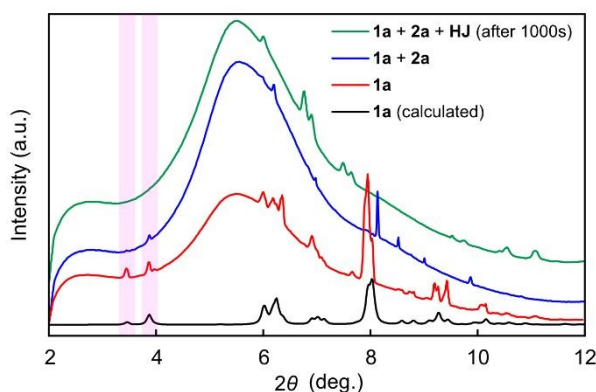


Fig. 2 In situ PXRD patterns of **1a**, **1a + 2a**, and **1a + 2a + HJ** during ball milling.

diffraction peaks were observed at $2\theta = 3.5$ and 3.9° (blue line, Fig. 2). These peaks were consistent with those obtained from the milling of **1a** alone (red line, Fig. 2) and calculated pattern of **1a** based on its crystal structure (black line).³⁶ Next, **HJ** was added to **1a + 2a**, and the Michael addition reaction was performed by ball milling (**1a + 2a + HJ**). After milling for 1000 s, the in situ PXRD pattern showed complete disappearance of diffraction peaks at $2\theta = 3.5$ and 3.9° (green line, Fig. 2). This clearly indicated that the nitroalkene **1a** initially reacted while remaining its solid crystalline domain, and finally amorphous reaction mixture was obtained after the Michael addition reaction with the ball mill.

Throughout the in situ PXRD analysis, the solid reactants (**1a**) initially existed in the present catalytic system in the ball mill. In this situation, mixing of reactants and catalyst might be severely limited under the solvent-less conditions. Using polymer-supported catalyst as a POLAG additive, substrate-polymer interactions would efficiently disperse the solid substrates and drastically accelerate the catalytic reactions.

Synthesis of polymer-supported HJ

To further enhance the efficiency of Michael addition reactions in the presence of solids, we designed polymer-supported **HJ** that can function as POLAG additives. The polymer catalysts were synthesized by free radical copolymerization (Fig. 3a). Styrene-type monomers containing **HJ** (**HJ monomer**) were synthesized according to the previous reports (for details, see ESI).^{32,33} As spacer monomers, styrene (**S**), styrene derivatives bearing a *tert*-butyl group (**tBuS**) or ethylene glycol moiety (**EGS**), or methyl methacrylate (**MMA**) were copolymerized with the **HJ monomer**. By varying the chemical structure and feed ratio of the spacer monomers, a series of polymer catalysts was prepared (**pHJ-S**, **pHJ-tBuS**, **pHJ-EGS**, **pHJ-S-tBuS**, **pHJ-S-EGS**, and **pHJ-MMA**) (Table S1†). All polymers were obtained as white or yellowish powder (28–69% yield). ¹H NMR analysis confirmed the incorporation of **HJ** into the polymers ($[\text{HJ}] = 0.39\text{--}1.29\text{ mmol g}^{-1}$, Fig. S9–14†). Size exclusion chromatography (SEC) analysis confirmed unimodal molecular weight distributions (8,900–38,300 g mol^{-1} , Fig. 3b and S15). DSC measurements for the polymers were performed to obtain glass transition temperature (T_g) (Fig. 3c). The T_g is a thermophysical property that correlates polymer chain

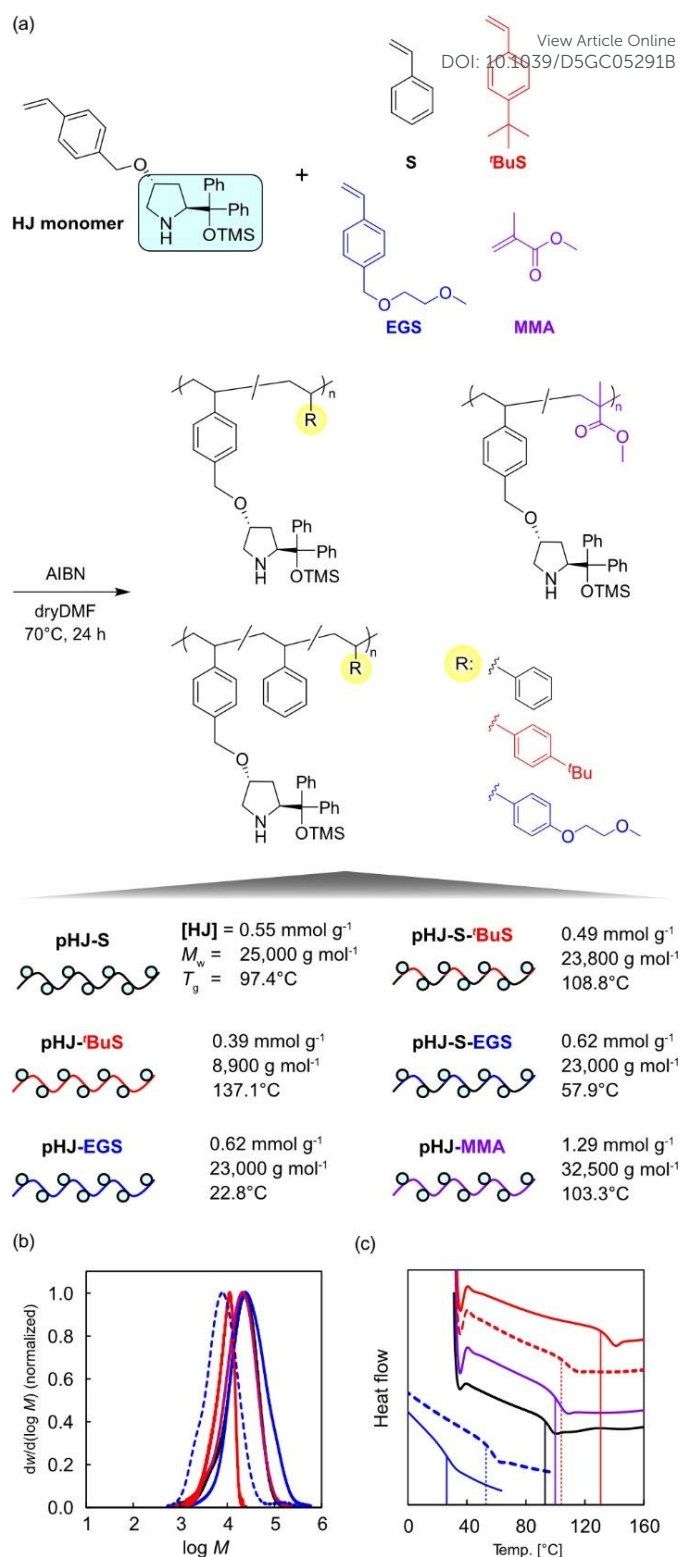


Fig. 3 (a) Synthesis of polymer-supported **HJ**. (b) SEC chromatogram of polymer-supported **HJ**. (c) DSC curves of polymer-supported **HJ** (second heating step). **pHJ-S** (solid black line), **pHJ-tBuS** (solid red line), **pHJ-EGS** (solid blue line), **pHJ-S-tBuS** (dashed red line), **pHJ-S-EGS** (dashed blue line), **pHJ-MMA** (solid purple line).

flexibility (lower T_g indicates higher polymer chain flexibility). The T_g of the polymer catalysts with different spacer structures ranged from 22.8 to 137.1°C, strongly depending on the chemical structure of spacer monomer and feed ratio. Notably,



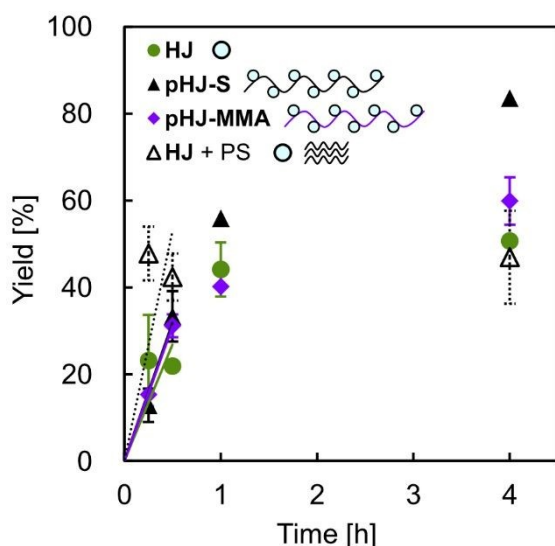


Fig. 4 Time-yield profile in solvent-less Michael addition using ball milling with HJ, pHJ-S, pHJ-MMA, and HJ + PS.

the introduction of ethylene glycol units dramatically lowered the T_g of the polymer catalyst (22.8 and 57.9°C for **pHJ-EGS** and **pHJ-S-EGS**, respectively). This suggested that the presence of flexible ethylene glycol structures enhanced polymer chain flexibility.³⁷

Effect of polymer backbones on catalytic performance

The Michael addition reaction was performed in the ball mill using the synthesized polymer-supported HJ. The **pHJ-S** and **pHJ-MMA**, which had comparable T_g (97.4 and 103.3°C), was first tested in the mechanochemical Michael addition reaction. A catalyst loading was fixed to be 1 mol% for high diastereoselectivity (Table 1). The mechanochemical reactions were performed in different batches with varying reaction times to obtain a time-yield profile (Fig. 4). All polymer catalysts showed comparable stereoselectivity with HJ (84:16–91:9 *syn/anti*, Table 2). In the initial reaction time (0.25 to 0.5 h), the yield increased almost proportionally with increasing the reaction time. Interestingly, in the initial reaction time, turnover frequencies (TOFs) of **pHJ-S** and **pHJ-MMA** (64 and 62 h⁻¹, respectively) were significantly higher than that of HJ (54 h⁻¹, Table 2). After 1 h, however, the reaction drastically slowed except for **pHJ-S** system. The turnover numbers (TONs) at reaction time of 4 h were 51, 84, and 68 for HJ, **pHJ-S**, and **pHJ-MMA**, respectively. It should be noted that the TON of the **pHJ-S** was 1.6-fold higher than that of HJ. No clear correlation was found between the catalytic activity and molecular weights and catalyst loadings in the **pHJ-S** system (Table S2 and S3[†]). When mixing the HJ and catalyst-free polystyrene (PS) as a POLAG additive (HJ + PS), HJ exhibited a high TOF (106 h⁻¹, Table 2), but the TON was still low (47).

As expected, the polymer backbone of catalyst functioned as a POLAG additive by effectively dispersing solid substrate to increase the contact efficiency between the reactants and catalyst to improve the TOF. It is noteworthy that the TON also dramatically increased by using **pHJ-S**. To gain insight into this

Table 2 Solvent-less Michael addition using ball milling with HJ and polymer-supported HJ^a

Catalyst	TOF [h ⁻¹] ^{b,c}	TON [-] ^b	<i>syn:anti</i> ^b
HJ	54	51	90:10-94:6
pHJ-MMA	62	68	88:12-91:9
pHJ-S	64	84	84:16-90:10
HJ + PS	106	47	91:9-95:5

^a Reaction condition: **1** (1.8 mmol, 1.0 eq.), **2** (3.6 mmol, 2.0 eq.) and catalyst (1 mol% as HJ unit) were milled in 20 mL ZrO₂ jar with four ZrO₂ balls (Φ = 10 mm) under an ambient atmosphere. ^b Determined by HPLC. ^c Determined at reaction time from 0.25 to 0.5 h.

amazingly high catalyst durability, the reaction mixture was analyzed by SEC and ¹H NMR spectroscopy after the catalytic reaction in the ball mill for 4 h. The SEC analysis of the spent **pHJ-S** found that the molecular weight remained almost the same before and after the reaction (Fig. S16[†]). On the other hand, drastic decrease in the ¹H NMR peak integral of methyl proton of TMS group on the HJ unit was observed (Fig. S17[†]). Based on the peak integral ratio of the TMS group to methylene proton on the five-membered ring of the HJ unit, it was confirmed that only 20 and 22% of the TMS groups remained in the spent HJ and **pHJ-MMA**, respectively. Surprisingly, 49% of the TMS groups remained in the spent **pHJ-S**.

From the ¹H NMR analyses, degradation of TMS group of HJ was suggested, while the **pHJ-S** showed the highest stability. During the catalytic cycle of the HJ in the asymmetric Michael addition reaction, nucleophilic attack of the N atom of HJ to the aldehyde occurs, which eliminates H₂O to form an enamine. If H₂O molecules in the reaction system hydrolyzed the TMS group, a parasitic oxazolidine might form from the enamine, leading to the subsequent stagnation of the catalytic cycle.^{38,39} In our system, immobilizing the HJ moiety on the polystyrene backbone (i.e. **pHJ-S**) suppressed the hydrolysis of the TMS group, resulting in an improved TON. From a comparison with **pHJ-MMA**, it was suggested that choice of appropriate polarity of polymer backbone was crucial to boost both the reaction rate and catalytic durability of water-labile organocatalyst in mechanochemical organic synthesis.

Effect of polymer side-chain structure on catalytic performance

The catalytic performance of polymer-supported HJ with different side-chain structures on polystyrene backbone (**pHJ-S**, **pHJ-^tBuS**, **pHJ-EGS**, **pHJ-S-^tBuS**, and **pHJ-S-EGS**) was further compared (Fig. 5 and Table S4). All the polymer-supported catalysts initiated the reaction while remaining as solids (Fig. S18[†]). The polymer catalysts showed higher TONs (76–>99, Fig. 5a, b, and Table S4) compared to HJ (Table 2). **pHJ-EGS** and **pHJ-S-EGS**, which had ethylene glycol moieties in their side chains, showed TOFs of 66 and 65 h⁻¹, respectively (Fig. 5b and Table S4). These TOFs were slightly higher than that of **pHJ-S** (64 h⁻¹ TOF). On the other hand, **pHJ-^tBuS** and **pHJ-S-^tBuS**, which had ^tBu-substituted phenyl rings, provided the low TOFs (48 and 46 h⁻¹, respectively). Through these comparative experiments, the polymer-supported HJ with low T_g (i.e., more flexible polymer chain) showed much higher TOFs. It is noteworthy that the **pHJ-S**



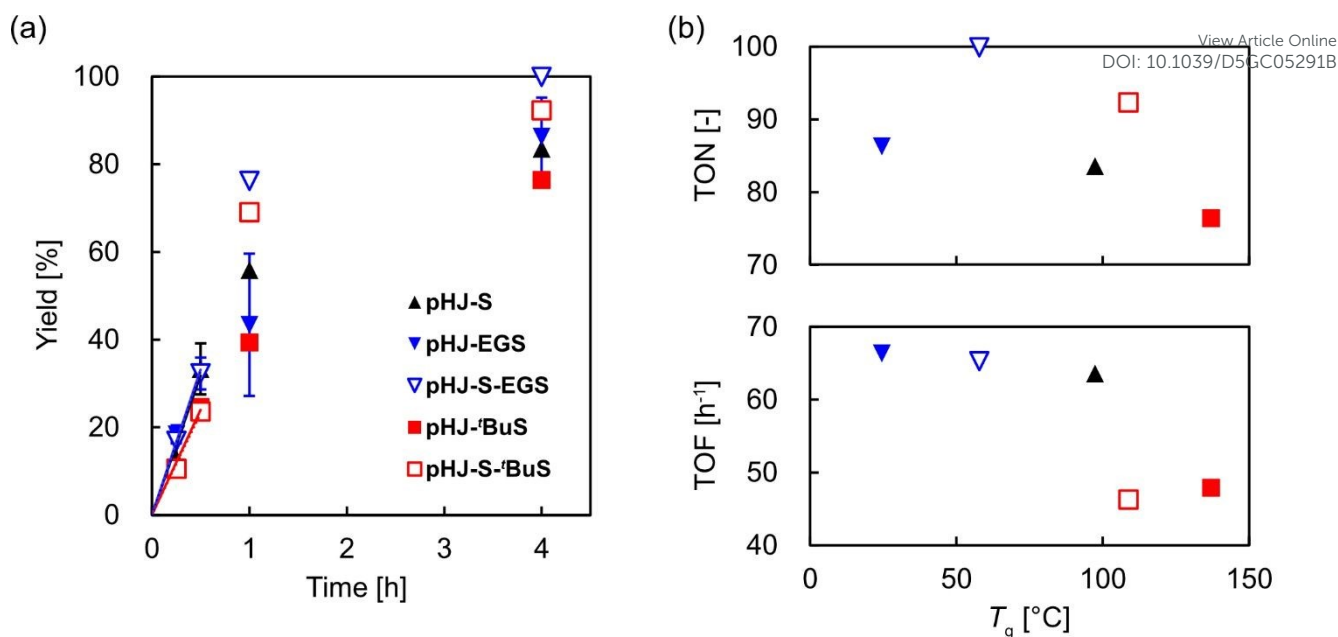


Fig. 5 (a) Time-yield profile in the Michael addition reaction with ball milling. (b) TOF and TON vs. T_g of polymer-supported **HJ** with different chemical structure of side chains.

S-EGS afforded desired product **3a** with high enantiomeric excess (ee) of 93%, while the unsupported **HJ** showed only 69% ee under the mechanochemical condition. Surprisingly, the flexible polymer catalysts accelerated the reaction in the mechanochemical Michael addition reaction.

Through the comparative experiments, the thermophysical property (T_g) of the polymer-supported **HJ** affected its TOF in the mechanochemical organic synthesis with the ball mill. The reaction acceleration with the flexible polymer catalyst was

probably due to the following two factors: (i) high mixing degree for solid dispersion and (ii) high contact efficiency between the reactants and catalytic site within the polymer phase (Fig. 6).

As for the (i), ball mill provided mechanical energy to abrade and mix solid reactants in the Michael addition reaction. Subsequently, the polymer catalyst functioned as POLAG additive to disperse the solid reactant. Compared with rigid polymer catalyst with high T_g , high flexibility of polymer catalyst with low T_g could promote the dispersion by mechanical deformation of its polymer chain to interact with newly generated surface of the solid reactants.⁴⁰

As for the (ii), the dispersed reactant should access the catalytic site within the polymer phase. It has been reported that solid-state modification of polymer with external reagents by the ball mill was pronounced within mobile polymer phase.^{41,42} These studies suggested that the flexible polymer with low T_g can smoothly accommodate external reactants in their polymer phase. Given this, the low- T_g polymer catalyst might utilize the input mechanical energy to deform its polymer chain, expose the active sites toward the external reactants, and facilitate the reactant access for reaction acceleration. The polymer flexibility was one of factors that determined catalytic efficiency in the solvent-less mechanochemical organic synthesis.

Substrate scope

Using the polymer-supported catalyst **pHJ-S-EGS**, we tested the substrate scope in the Michael addition reactions. The reaction of **2a** with 4-bromo-(E)- β -nitrostyrene (**1b**) or 4-methoxy-(E)- β -nitrostyrene (**1c**) afforded corresponding products (**3b** and **3c**) with high yields (80 and 75%) and stereoselectivity (80:20 and 85:15 *syn/anti*, Table S5[†]). The small molecular counterpart (**HJ**) showed low yields of **3b** and **3c** (56 and 34% respectively), which emphasized the superiority of the polymer-supported **HJ** system. When bulky aldehydes were used, the product was

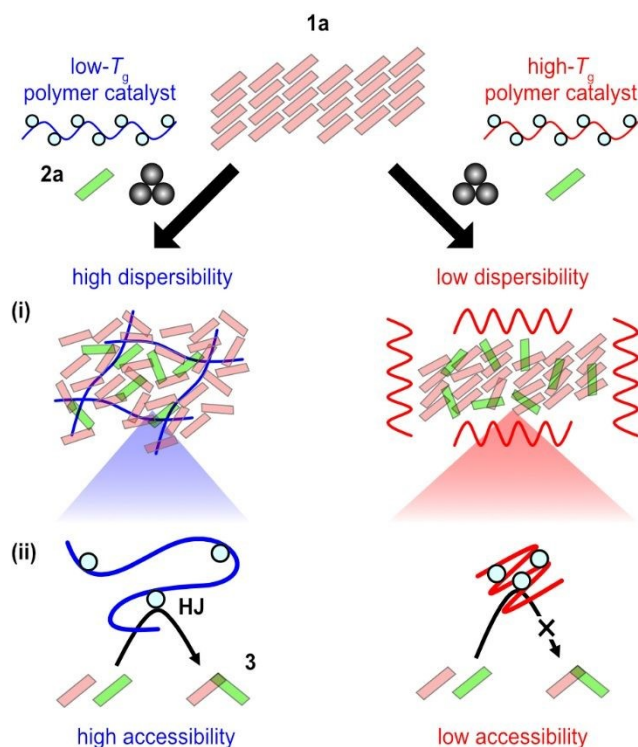
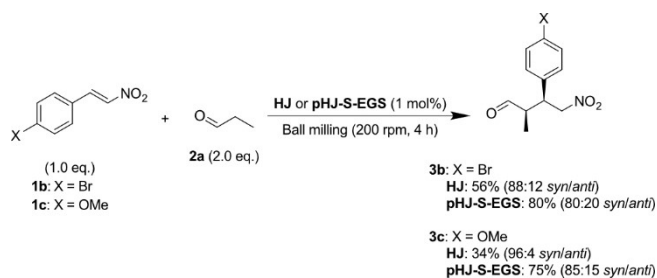


Fig. 6 Schematic of (i) high mixing degree for solid dispersion and (ii) high contact efficiency between the reactants and catalytic site within the polymer phase.





Scheme 1 Solvent-less asymmetric Michael addition reaction of substituted nitrostyrene using ball milling. Reaction condition: **1b** or **1c** (1.8 mmol, 1.0 eq.), **2a** (3.6 mmol, 2.0 eq.), and catalyst (1 mol% as **HJ** unit) were milled in 20 mL ZrO₂ jar with four ZrO₂ balls (Φ = 10 mm) under ambient atmosphere. Yields and diastereoselectivity were determined by ¹H NMR (xylene was used as an internal standard).

obtained in significantly lower yields (Table S5[†]). This was likely due to inhibition of the enamine formation in the catalytic cycle of the **HJ**. Throughout the screening of the scope, it was demonstrated that the excellent catalytic activity of the polymer-supported **HJ** for various nitrostyrene.

Evaluation of green metrics

Finally, the utility of polymer-supported **HJ** was further emphasized by comparison of various green metrics such as E-factor, PMI, and SI (Fig. 7). For all the metrics, smaller value is more desirable from a green chemistry perspective.⁴³ While the values for the solution system (Solution (**HJ**)) exceeded 50 for all the metrics, the mechanochemical systems using ball milling catalyzed by **HJ** and **pHJ-S-EGS** (**Ball milling (HJ)** and **Ball milling (pHJ-S-EGS)**) showed significantly smaller values (<2) because no solvent was used in the reaction. In the unsupported catalyst system, some of the substrates remained unreacted due to catalyst deactivation, which still needed purification of the reaction mixture to obtain pure product **3**. On the other hand, since almost all the substrate was converted using polymer-supported catalyst system, all the metric values for **Ball milling (pHJ-S-EGS)** were even smaller (0.1–1.1) compared to those for **Ball milling (HJ)** (1.0–2.0), respectively. These findings in green

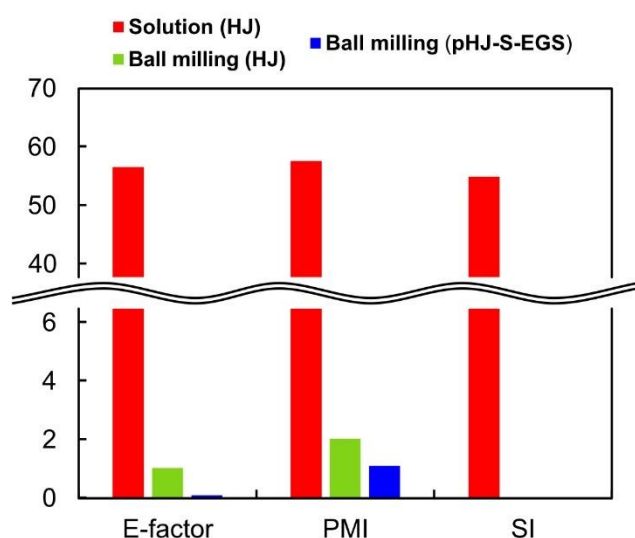


Fig. 7 Summary of green chemistry metrics. PMI = process mass intensity, SI = solvent intensity.

metrics underscored the importance of solvent-less conditions and choice of catalyst support for more efficient and greener mechanochemical synthesis.

Conclusion

In this study, the influence of the structure of polymer-supported catalysts on their catalytic activity in mechanochemical organic synthesis was investigated in the presence of solid reactant. The TOF and TON were boosted by addition of polymer as POLAG additive and choice of appropriate polymer backbone for supported catalysts. Interestingly, a correlation was observed between the *T_g* of the polymer and the TOF. This indicates that the thermophysical properties of the polymer support governed catalytic activity in mechanochemical organic synthesis. Furthermore, the superiority of using polymer-supported catalysts was demonstrated based on green chemistry metrics. The design guidelines of polymer-supported catalysts for mechanochemical organic synthesis are expected to accelerate the development of highly efficient and more sustainable fine chemical synthesis processes under solvent-less reaction conditions.

Author contributions

We greatly appreciate Prof. Dr Inoue at Kyushu University for providing planetary mill and supporting experiments with the ball mill. KH, HM, and YM designed the experiments. KH performed experiments. HK and EN supported in situ PXRD measurement. KH, HM, and YM wrote the manuscript. MN, HK, and EN contributed to discussions during this work. All authors have read and approved the final version of manuscript.

Conflicts of interest

There are no conflicts to declare.

Data availability

The authors confirm that the data supporting the findings of this study are available within the article and its ESI[†] materials.

Acknowledgements

This work was supported by JSPS KAKENHI grant numbers JP24K17560, JP23K26708, the Environment Research and Technology Development Fund (JPMEERF20255RB4) of the Environmental Restoration and Conservation Agency (ERCA) provided by Ministry of the Environment of Japan, the Sumitomo Foundation, the Yashima Environment Technology Foundation, and the Tobemaki Foundation. This article is based on results obtained from a project, JPNP20004, subsidized by New Energy and Industrial Technology Development Organization (NEDO). The synchrotron experiments were performed at SPring-8 BL13XU with the approval of the Japan



Synchrotron Radiation Research Institute (JASRI) (Proposal No. 2024B1782 and 2024B1977).

References

- 1 P. Anastas, M. Nolasco, F. Kerton, M. Kirchhof, P. Licence, T. Pradeep, B. Subramaniam and A. Moores, *ACS Sustainable Chem. Eng.*, 2021, **9**, 8015–8017.
- 2 D. J. C. Constable, C. Jimenez-Gonzalez and R. K. Henderson, *Org. Proc. Res. Dev.*, 2007, **11**, 133–137.
- 3 C. Jimenez-Gonzalez, C. S. Ponder, Q. B. Broxterman and J. B. Manley, *Org. Proc. Res. Dev.*, 2011, **15**, 912–917.
- 4 R. A. Sheldon, *Green Chem.*, 2017, **19**, 18–43.
- 5 G. W. Wang, *Chem. Soc. Rev.*, 2013, **42**, 7668.
- 6 T. K. Achar, A. Bose and P. Mal, *Beilstein J. Org. Chem.*, 2017, **13**, 1907–1931.
- 7 V. Némethová, D. Křištofiková, M. Mečiarová and R. Šebesta, *Chem. Rec.*, 2023, **23**, e202200283.
- 8 K. Kubota, *Bull. Chem. Soc. Jpn.*, 2023, **96**, 913–930.
- 9 D. Braga, L. Maini and F. Grepioni, *Chem. Soc. Rev.*, 2013, **42**, 7638–7648.
- 10 Y. Xiao, C. Wu, X. Hu, K. Chen, L. Qi, P. Cui, L. Zhou and Q. Yin, *Cryst. Growth Des.*, 2023, **23**, 4680–4700.
- 11 A. Krusenbaum, S. Grätz, G. T. Tigineh, L. Borchardt and J. G. Kim, *Chem. Soc. Rev.*, 2022, **51**, 2873–2905.
- 12 J. Li, C. Nagamani and J. S. Moore, *Acc. Chem. Res.*, 2015, **48**, 2181–2190.
- 13 A. Taghipour, A. Rahimpour, M. Rastgar and M. Sadrzadeh, *Ultrason. Sonochem.*, 2022, **90**, 106202.
- 14 J. Andersen and J. J. Mack, *Green Chem.*, 2018, **20**, 1435.
- 15 Q. T. Trinh, N. Golio, Y. Cheng, H. Ha, K. U. Tai, L. Ouyang, J. Zhao, T. S. Tran, T. K. Nguyen, J. Zhang, H. An, Z. Wei, F. Jerome, P. N. Amaniampompong and N. T. Nguyen, *Green Chem.*, 2025, **27**, 4926.
- 16 A. Stolle, T. Szuppa, S. E. S. Leonhardt and B. Ondruschka, *Chem. Soc. Rev.*, 2011, **40**, 2317–2329.
- 17 J. G. Hernández and C. Bolm, *J. Org. Chem.*, 2017, **82**, 4007–4019.
- 18 Z. J. Jiang, Z. H. Li, J. B. Yu and W. K. Su, *J. Org. Chem.*, 2016, **81**, 10072–10078.
- 19 K. Kubota, T. Seo, K. Koide, Y. Hasegawa and H. Ito, *Nat. Commun.*, 2019, **10**, 111.
- 20 P. Ying, T. Ying, H. Chen, K. Xiang, W. Su, H. Xie and J. Yu, *Org. Chem. Front.*, 2024, **11**, 127–134.
- 21 A. M. Belenguer, G. I. Lampronti, A. J. Cruz-Cabeza, C. A. Hunter and J. K. M. Sanders, *Chem. Sci.*, 2016, **7**, 6617–6627.
- 22 A. Mascitti, M. Lupacchini, R. Guerra, I. Taydakov, L. Tonucci, N. d'Alessandro, F. Lamaty, J. Martinez and E. Colacino, *Beilstein J. Org. Chem.*, 2017, **13**, 19–25.
- 23 L. Konnert, M. Dimassi, L. Gonnet, L. Lamaty, F. Martinez and E. Colacino, *RSC Adv.*, 2016, **6**, 36978.
- 24 V. Declerck, E. Colacino, X. Bantreil, J. Martinez and F. Lamaty, *Chem. Commun.*, 2012, **48**, 11778–11780.
- 25 K. Kubota, T. Seo and H. Ito, *Faraday Discuss.*, 2023, **241**, 104.
- 26 T. Seo, K. Kubota and H. Ito, *J. Am. Chem. Soc.*, 2023, **145**, 6823–6837.
- 27 K. Xiang, H. Shou, C. Hu, W. Su and J. Yu, *Green Chem.*, 2024, **26**, 5890.
- 28 Y. Hayashi, H. Gotoh, T. Hayashi and M. Shoji, *Angew. Chem., Int. Ed.*, 2005, **44**, 4212–4215.
- 29 K. A. Jørgensen, M. Johannsen, S. Yao, H. Audrain and J. Thorhauge, *Acc. Chem. Res.*, 1999, **32**, 605–613.
- 30 M. Pagliaro, V. Pandarus, R. Ciriminna, F. Bland and P. D. Carà, *ChemCatChem*, 2012, **4**, 1013–1018.
- 31 Y. Hayashi, S. Hattori and S. Koshino, *Chem. – Asian J.*, 2022, **17**, e202200314.
- 32 H. Ochiai, A. Nishiyama, N. Haraguchi and S. Itsuno, *Org. Process Res. Dev.*, 2020, **24**, 10, 2228–2233.
- 33 H. Shigeeda, H. Matsumoto, M. Nagao and Y. Miura, *React. Chem. Eng.*, 2025, **10**, 1038–1046.
- 34 Y. Zheng, H. Kasai, S. Kobayashi, S. Kawaguchi and E. Nishibori, *Mater. Adv.*, 2023, **4**, 1005–1010.
- 35 Y. Yano, H. Kasai, Y. Zheng, E. Nishibori, Y. Hisada and T. Ono, *Angew. Chem., Int. Ed.*, 2022, **61**, e202203853.
- 36 J. Haraada, M. Harakawa and K. Ogawa, *CrystEngComm* 2009, **11**, 638–642.
- 37 L. Zahir, N. J. Ara and S. I. Chowdhury, *Chem. Sci. Eng. Res.*, 2020, **2**, 34–38.
- 38 M. B. Schmid, K. Zeiter and R. M. Gschwind, *J. Am. Chem. Soc.*, 2011, **133**, 7065–7074.
- 39 O. V. Maltsev, O. A. Chizhov and S. G. Zlotin, *Chem. Eur. J.*, 2011, **17**, 6109–6117.
- 40 C. Asgreen, M. M. Knopp, J. Skytte and K. Löbmann, *Pharmaceutics*, 2020, **12**, 483.
- 41 Gerbehaye, C., Bernaerts, K. V., Mincheva, R. and Raquez, J. M., *Eur. Polym. J.*, 2022, **166**, 111010.
- 42 Bravo, J. J. P., Gerbehaye, C., Raquez, J. M. and Mincheva, R., *Molecules*, 2024, **29**, 667.
- 43 N. Fantozzi, J. N. Volle, A. Porcheddu, D. Virieux, F. García and E. Colacino, *Chem. Soc. Rev.*, 2023, **52**, 6680–6714.



View Article Online
DOI: 10.1039/D5GC05291B

Data availability

The authors confirm that the data supporting the findings of this study are available within the article and its ESI† materials.

